

# Determination of the ion beam energy width in tandem Van de Graaff accelerators via Auger projectile spectroscopy

S. Nanos<sup>a,b</sup>, A. Biniskos<sup>a</sup>, A. Laoutaris<sup>b,c</sup>, M. Andrianis<sup>b</sup>, T.J.M. Zouros<sup>c</sup>, A. Lagoyannis<sup>b</sup>, E.P. Benis<sup>a,\*</sup>

<sup>a</sup> Department of Physics, University of Ioannina, GR-45110 Ioannina, Greece

<sup>b</sup> Tandem Accelerator Laboratory, INPP, NCSR “Demokritos”, GR-15310 Ag. Paraskevi, Greece

<sup>c</sup> Department of Physics, University of Crete, GR-70013 Heraklion, Greece

## ARTICLE INFO

### Keywords:

Beam diagnostics  
Ion beam energy width  
Accelerators  
Auger  
SIMION

## ABSTRACT

Fast ion beams delivered by tandem Van de Graaff accelerators intrinsically have an energy width,  $\Delta E_p/E_p$ , due to the voltage ripple of the accelerator, the production mechanism of the highly charged ions inside the tank of the accelerator, as well as geometrical considerations related to the propagation of the ion beam. The ion beam energy width directly affects the experimental resolution and thus its value should be considered in experiments and the corresponding data analysis. Here, we present a method for determining the energy width of ion beams delivered by tandem Van de Graaff accelerators, based on high resolution Auger projectile electron spectroscopy combined with data analysis via Monte Carlo simulations within the SIMION ion optics package.

## 1. Introduction

The production of positively charged ions in tandem Van de Graaff accelerators is achieved by passing the initially negatively charged ion beam through a gas or foil medium (termed stripping medium or simply stripper) located at the maximum voltage area inside the accelerator's terminal. Upon collision of the negative ions with the gas or foil stripper, several electrons can be removed from the ion, thus resulting in a charge distribution of positively charged ions. The positively charged ions exit the terminal of the accelerator with a kinetic energy,  $E = (q + 1)V$ , where  $q$  is the charge state of the ion and  $V$  is the maximum voltage of the accelerator. Depending on the stripping medium type, i.e. gas or foil, the stripping process is widely known as *gas terminal stripping* (GTS) or *foil terminal stripping* (FTS), respectively.

The charge states resulting from the stripping process follow Gaussian-like distributions, the maximum value and width of which depend on the incoming charge state, the stripping energy and the stripping medium. Higher charge states, residing at the high end of the distribution, and thus delivered with very low current, can be reached by applying a second stripping process. This process takes place between the analyzing and the switching magnet of the beamline manifold of the accelerator, and is termed *post-stripping*. In this case, an ion beam with a selected charge state at a certain energy collides with a gas or foil target thus resulting in a new charge state distribution that

is shifted to higher charge state values as compared to the initial one. This is because the stripping now takes place at the much higher energy after acceleration in the tandem Van de Graaff. Similarly, depending on the stripping medium, gas or foil, the post-stripping process is known as *gas post-stripping* (GPS) or *foil post-stripping* (FPS), respectively.

The estimation of the ion beam current at a certain charge state and energy is necessary for the design of an experiment. For this, several software packages have been developed based on semiempirical models and approaches [1–4]. Thus, charge state distributions can be quite accurately estimated by varying: (i) the incoming charge state, (ii) the stripping energy, (iii) the stripping medium, and (iv) the stripping location. However, they do not provide information about the ion beam energy width.

The ion beam energy width is a parameter that should be considered in experiments, as it affects the energy resolution of the measurements. In general, gas stripping results in narrower energy width than foil stripping. This is attributed to the energy straggling of the beam inside the thin foils, which also results in a small reduction of the initial kinetic energy. Thus, even though the use of gas stripping seems the apparent choice, in certain cases foil stripping is preferable for the generally higher currents or for avoiding the use of cumbersome differential pumping schemes. In all cases, the knowledge of the energy width of the ion beam is an important parameter for the data analysis, and should be known with accuracy.

\* Corresponding author.

E-mail address: [mbenis@uoi.gr](mailto:mbenis@uoi.gr) (E.P. Benis).

<https://doi.org/10.1016/j.nimb.2023.05.027>

Received 22 March 2023; Received in revised form 2 May 2023; Accepted 7 May 2023

Available online 18 May 2023

0168-583X/© 2023 Elsevier B.V. All rights reserved.

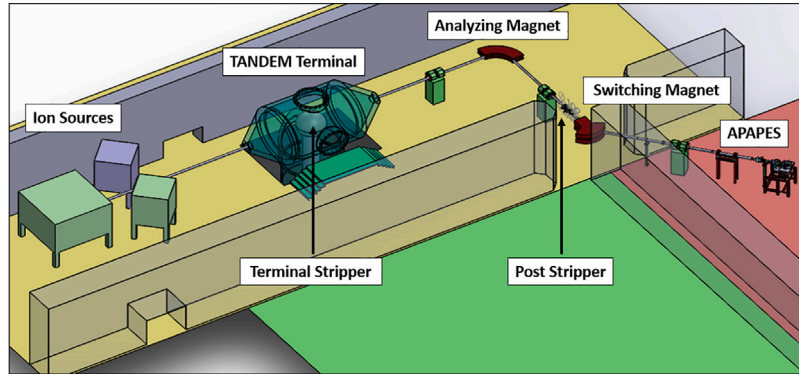


Fig. 1. CAD view of the tandem Van de Graaff accelerator laboratory of NCSR “Demokritos”, depicting only the main accelerator components and the location of the APAPES setup.

There are several techniques widely used in tandem accelerator facilities for determining the energy width of a beam, such as beam current measurement [5], beam profile monitors [6], and nuclear resonances [7]. In beam current measurements, Faraday cups are used to measure the beam current at different energies in order to infer the energy width of the beam. Beam profile monitors are used to obtain the spatial distribution of the beam, from which the energy width can be obtained. Nuclear resonances involve the  $\gamma$ -ray yield measurement of strong and narrow  $(p, \gamma)$  or  $(p, p'\gamma)$  reactions. The energy width of the beam is determined by the deconvolution of the measured yield taking into account the intrinsic resonance width [8].

Here, we present an alternative way for determining the energy width of the ion beams delivered by tandem Van de Graaff accelerators. The method is based on measurements of state-selective projectile Auger electron spectra analyzed with Monte Carlo simulation approaches realized within the SIMION ion optics package [9]. It is an *in situ* method since the ion beam energy width is convoluted within the Auger electron spectra and thus does not necessitate additional measurements. Moreover, all the parameters that affect the energy width, such as the stripping location and the settings of the slits of the accelerator or the beamline of the experimental setup, are allowed to be varied for each experiment, since the energy width can be obtained for each experiment independently.

## 2. Experiment

The experiments were conducted at the APAPES beamline (Atomic Physics with Accelerators: Projectile Electron Spectroscopy [10]), located at the laboratory of the tandem Van de Graaff 5.5 MV accelerator in NCSR “Demokritos” [11]. The accelerator has recently been equipped with an inbuilt post-stripping device [12], supporting both GPS and FPS, installed in the area between the analyzing and the switching magnets, as shown in Fig. 1. Thus, highly charged ion beams, necessary for atomic physics experiments, inaccessible by single-step stripping, are now available. The ion beam charge state distribution and corresponding relative currents are estimated using the software package TARDIS that has been developed for the tandem accelerator of “Demokritos” [13].

The APAPES beamline has been developed to support atomic physics studies based on high resolution projectile electron spectroscopy. The latter requires measurements of projectile electrons emitted at zero degrees with respect to the projectile velocity, a technique widely known as ZAPS (zero-degree Auger projectile spectroscopy) [14,15]. The APAPES beamline hosts an electron spectrograph consisting of an electrostatic single-stage hemispherical detector analyzer (HDA) equipped with a four-element injection lens and a two-dimensional position sensitive detector (PSD). The projectile passes through a doubly differentially pumped gas cell where it interacts with the gas target. After exiting the cell, the ion beam continues through

the spectrograph to be collected in a Faraday cup for normalization purposes. The electrons emitted at zero degrees with respect to the ion beam velocity are focused by the entry lens and energetically analyzed by the HDA and imaged on the PSD. The detailed operation of the ZAPS setup at the tandem laboratory of “Demokritos” has been reported in previous publications of our research team [16,17].

High resolution projectile spectroscopy provides measurements of doubly differential in energy and solid angle cross-sections (DDCS). In ZAPS, the laboratory frame DDCS is determined according to the following equation [18]:

$$DDCS_j = \frac{d^2\sigma_j}{d\Omega dE_j} = \frac{N_j^e}{N_I L_{eff} n \Delta\Omega \Delta E_j T \eta} \quad (1)$$

where  $N_j^e$  is the number of electrons detected in channel  $j$ ,  $N_I$  is the number of ions collected in the Faraday cup,  $L_{eff}$  is the effective length of the target gas cell,  $n$  is the target gas density,  $\Delta\Omega$  is the solid angle,  $\Delta E_j$  is the energy step per channel in the spectrum, and  $T$  is the analyzer transmission. The overall efficiency,  $\eta$ , is determined from measurements of binary encounter electron peaks [19]. The laboratory frame DDCS can be transformed to the projectile rest frame according to the kinematics transformation [18]:

$$\frac{d^2\sigma}{d\Omega' d\epsilon'} = \frac{d^2\sigma}{d\Omega d\epsilon} \sqrt{\frac{\epsilon'}{\epsilon}} \quad (2)$$

where primed symbols denote the quantities in the projectile rest frame. The electron kinetic energy  $\epsilon'$  in the projectile rest frame is related to the corresponding kinetic energy in the laboratory frame  $\epsilon$  for zero-degree emission as [18]:

$$\epsilon'(t_p, \epsilon) = \epsilon + t_p - 2\sqrt{\epsilon t_p} \quad (3)$$

with

$$t_p = \frac{m}{M_p} E_p = 548.58 \frac{E_p(\text{MeV})}{M_p(\text{u})} (\text{eV}) \quad (4)$$

being the reduced projectile energy known also as the *cusp* electron energy (electrons isotachic to the projectile) [19].  $E_p$  and  $M_p$  are the kinetic energy and mass of the projectile, respectively, while  $m$  is the electron mass.

In this study, highly charged oxygen beams were used in collisions with helium targets to obtain the KLL Auger spectra. In Fig. 2, typical KLL Auger spectra, obtained for the collision system of 11 MeV  $\text{O}^{6+} + \text{He}$  are presented. The incoming He-like  $\text{O}^{6+}$  forms transient Li-like doubly excited states through the processes of single electron transfer [20] or electron transfer and excitation [21], which subsequently deexcite through KLL Auger decay. The two KLL Auger spectra, shown in Fig. 2, correspond to the  $\text{O}^{6+}$  beams resulting from post-stripping the  $\text{O}^{4+}$  beam, selected by the analyzing magnet, onto either gas (GPS) or thin carbon foils (FPS). The thin carbon foils were developed at the tandem Van de Graaff laboratory of “Demokritos” and had a typical

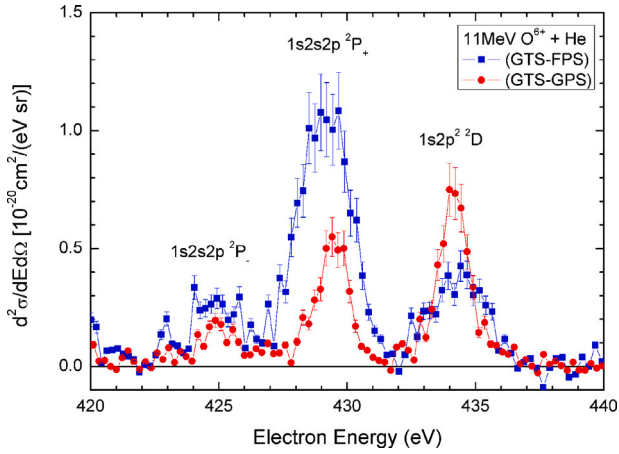


Fig. 2. DDCS electron spectra for the collision system 11 MeV  $O^{6+} + He$ , showing the effect of the stripping method on the Auger line widths. Blue filled squares: GTS-FPS; Red filled circles: GTS-GPS.

density of about  $50 \mu\text{g}/\text{cm}^2$ , while the gas target in use was  $N_2$ . For both cases, the  $O^{4+}$  beams resulted from stripping the  $O^-$  ions in the gas terminal stripper (GTS). The different Auger peaks ratios, evident in Fig. 2, originate from the different configurations fractions of the ions delivered in the  $O^{6+}(1s^2 1S, 1s2s^3S)$  mixed-state, as resulting from the different stripping methods, i.e., FPS or GTS [22]. From Fig. 2 it is clearly seen that foil stripping results in broader KLL Auger peaks due to the broader energy width of the  $O^{6+}$  ion beam.

### 3. SIMION simulations

In the proposed method, the determination of the ion beam energy width is achieved by comparing the measured KLL Auger line widths with the corresponding ones obtained from Monte Carlo type simulations performed within the SIMION charge particle optics package [9]. For this, we modeled the ZAPS experimental setup geometry in SIMION, using the geometry design environment, with a design accuracy of 0.254 mm per grid unit, adequate for our studies as resulted from earlier similar SIMION investigations of the optical properties of the ZAPS setup [23,24].

In addition, a numerical code was built in the Lua programming language to simulate the electron emission and the measurement process. There, a large number (typically  $\sim 10^5$ – $10^6$ ) electron trajectories are generated from random positions within the gas cell area with Auger energies corresponding to the experimental ones and random solid angles limited by the detection geometry. This way, the electron emission process following the interaction of the ion beam with the gas target is simulated in accordance to a Monte Carlo type approach. In a next step, the electrons that are detected on the PSD area are used to obtain the energy spectrum after considering the spectrograph operation voltages and the energy calibration process. Finally, the spectra are transformed to the projectile frame following the laboratory frame transformations of Eq. (2), for a direct comparison with the corresponding DDCS measurements. A detailed presentation of the ZAPS spectrometer and related measurements simulated in SIMION can be found in [23–25].

In this study, the values of all the experimental and theoretical parameters were inserted into the code with a high accuracy. Geometrical dimensions were considered in the finest possible detail and the values of the spectrometer voltages were accurately measured with an accuracy better than 0.1%. In addition, the Auger energies and the lifetimes of the Li-like doubly-excited states ( $1s2s2l^{2,4}L$ ) involved were taken from Refs. [24,26]. The Auger energy distributions, the width of which was determined from their lifetime, were simulated

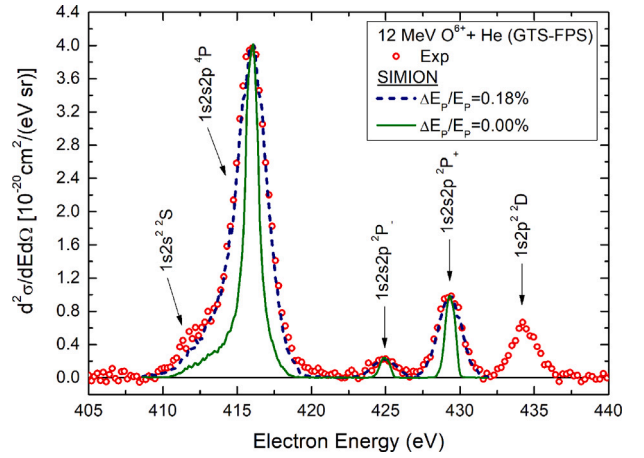


Fig. 3. Projectile rest frame zero-degree DDCS for the collision system of 12 MeV  $O^{6+} + He$ . Symbols: Experiment. Error bars are included in the magnitude of the symbol.; Lines: SIMION simulations for  $\Delta E_p/E_p = 0.18\%$  (dashed blue line) and for  $\Delta E_p/E_p = 0.00\%$  (full green line). Simulations were normalized to the measurements.

with pseudo-random Lorentzian distributions. Thus, the only parameter in the code that was treated as a free parameter was the beam energy width,  $\Delta E_p/E_p$ . A Gaussian pseudo-random distribution was used to simulate the energy width for the ion beam energy.

### 4. Data analysis

The data analysis was based on the comparison of the simulated spectra to the experimental ones in the projectile rest frame. Thus, for each experimental DDCS measurement of an Auger spectrum, we performed a series of SIMION runs by varying the parameter of ion beam energy width while keeping all the other parameters constant. In order to compare the simulated spectra with the experimental ones, we normalize their maximum Auger peak value to the experimental one. Such a comparison is presented in Fig. 3. There, it is clearly seen that, by using zero energy width for the energy of the ion beam, the simulated Auger spectra result in an energy resolution about half that of the experimental one. However, when the energy width is set to  $\Delta E_p/E_p = 0.18\%$ , the two spectra, simulated and experimental, show the best agreement, determined by the minimization of the sum of the residuals. It should be noted, that the result for the zero beam energy width corresponds to the convolution of the Auger states natural widths and the kinematic broadening [18], detailed below, with the response function of the spectrometer.

It is worth mentioning that the asymmetry of the  $1s2s2p^4P$  peak is due to the different lifetimes of its three  $J$ -levels [24]. Thus, every  $J$ -level was simulated separately, and the final distribution  $S^{(4P)}$  was obtained after statistically averaging over all the three  $J$ -levels, i.e.:

$$S^{(4P)} = \sum_J \frac{(2J+1)}{\sum_J (2J+1)} S^{(4P_J)}. \quad (5)$$

The result of the simulated  $1s2s2p^4P$  peak signal is presented in Fig. 4. Note that the asymmetry of the peak, originating from the different lifetimes of the three  $J$ -levels, is accurately reproduced in our modeling in SIMION, as evident in Fig. 3.

### 5. Results and discussion

In Fig. 5 we present our results about the values of the  $O^{6+}$  beam energy widths,  $\Delta E_p/E_p$ , obtained with the above described method, for collision energies ranging from 8 to 24 MeV. For higher energies ( $E_p > 18$  MeV) single-step GTS and FTS stripping processes were used, since at these high energies the ion beam current delivered at our

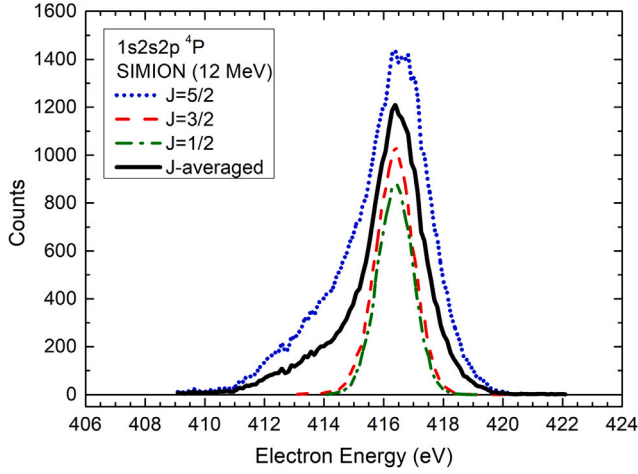


Fig. 4. SIMION simulation of the  $1s2s2p^4P$  Auger peak distribution for collision energy of 12 MeV. Contributions from the different  $J$ -levels as well as their statistical average are shown. Blue dashed line:  $J = 5/2$ ; Red dash-dotted line:  $J = 3/2$ ; Green dotted line:  $J = 1/2$ ; Black solid line: statistical sum.

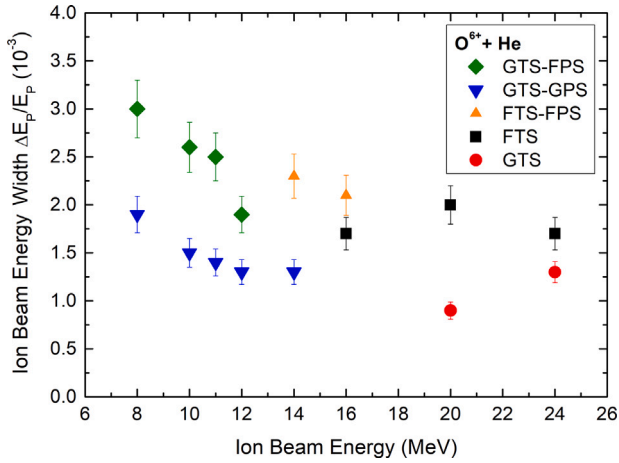


Fig. 5.  $O^{6+}$  ion beam energy width,  $\Delta E_p/E_p$ , obtained for collisions of 8–24 MeV  $O^{6+} + He$ . Different symbols refer to different beam stripping processes: Green filled diamonds, GTS-FPS; Blue filled down-pointing triangles, GTS-GPS; Orange filled up-pointing triangles, FTS-FPS; Black filled squares, FTS; Red filled circles, GTS.

experimental setup was of the order of a few nA, adequate for KLL Auger measurements. For lower energies, the ion beam current was too low for efficient measurements, and thus we used two-step stripping processes, the second being GPS or FPS.

The uncertainty of the method can be estimated by obtaining the lower and upper limits of  $\Delta E_p/E_p$  of the corresponding SIMION generated distributions that marginally include the experimental distribution. This way, an average uncertainty value of 10% was estimated for all the measurements, considering that all the KLL Auger spectra were recorded with high statistics, necessary for the valid application of our method.

From Fig. 5, it is evident that the energy width is broader for foil strippers, as expected based on energy straggling arguments mentioned above. The ion beam energy width shows an overall decrease with increasing collision energy independent of the stripping method. It should be emphasized that for all measurements, the pair of slits prior and after the analyzing magnet, that largely determine the ion beam energy and geometrical energy width were kept constant.

Our study was extended to include also  $O^{4+}$  beams. Thus, the same KLL Auger peaks were measured for the collisions of 12–20 MeV  $O^{4+} +$

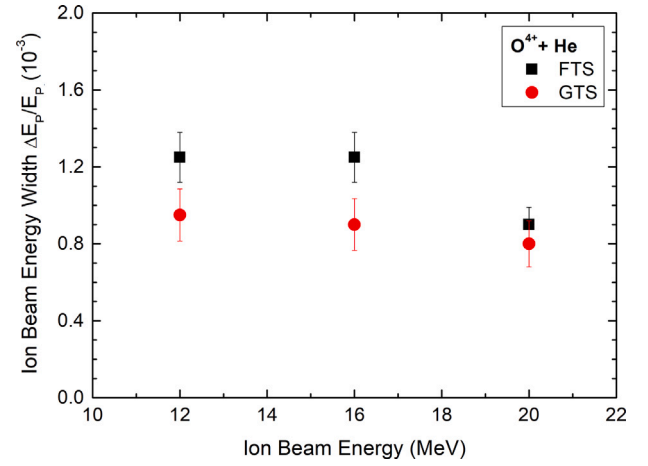


Fig. 6.  $O^{4+}$  ion beam energy width,  $\Delta E_p/E_p$ , obtained for collisions of 12–20 MeV  $O^{4+} + He$ . Different symbols refer to different beam stripping processes: Black filled squares, FTS; Red filled circles, GTS.

He. For these measurements only the single-step stripping inside the tandem accelerator was used, GTS and FTS, respectively. The results are presented in Fig. 6, where it is evident that the ion beam energy width shows an overall decrease with increasing collision energy independent of the stripping method, in accordance with the case of  $O^{6+}$  beams. However, the values of  $\Delta E_p/E_p$ , are overall smaller for the  $O^{4+}$  than for the  $O^{6+}$  beams. This is attributed to the higher terminal voltages used for the production of the  $O^{4+}$  beams (it is  $V = E/(q+1)$ ), and thus to their higher stripping collision energies.

Our results are in overall good agreement with the corresponding results from the nuclear resonances technique, widely used in nuclear experiments at the tandem Van de Graaff accelerator facility of NCSR “Demokritos” [7]. However, a direct comparison is not viable as the results are obtained from experiments performed at different beamline setups corresponding to different beam transportation conditions.

It should be noted that in our technique all the parameters that cause the broadening of the Auger peaks are included in the simulation and do not have to be determined independently. The advantage of the proposed approach is that in the ZAPS technique the effects of line broadenings are minimized. ZAPS is inherently a high resolution technique primarily due to the zero-degree detection angle. The kinematic broadening due to the finite entry solid angle of the spectrometer,  $\Delta\theta$ , is estimated to be in first order [18]:

$$\Delta B_{\theta}^{(1)} = -2 \sin \theta \Delta \theta \left( \frac{\sqrt{\epsilon' t_p}}{1 - \sqrt{\frac{\epsilon'}{t_p}} \cos \theta} \right). \quad (6)$$

For zero-degree observation the first order term vanishes, thus favoring the measurements at this angle, as the ZAPS technique does. The second order broadening is then estimated to be [18]:

$$\frac{\Delta B_{\theta}^{(2)}}{\epsilon'} = \left( 1 + \sqrt{\frac{t}{\epsilon'}} \right) \sqrt{\frac{t}{\epsilon'}} \left( \frac{\Delta \theta}{2} \right)^2. \quad (7)$$

The value of this term, estimated for an ion beam of 1 MeV/u and for an Auger energy of  $\epsilon' = 430$  eV, results in a contribution to the broadening of the Auger peak of only  $\frac{\Delta B_{\theta}^{(2)}}{\epsilon'} \approx 3 \times 10^{-3} \%$ .

In addition, the natural widths of the Auger peaks, as resulting from their lifetimes determined theoretically, are of the order of meV or smaller. In Table 1, we present the lifetimes and corresponding natural widths of the  $1s2s2p^2, ^4P$  states for  $O^{5+}$ , concerning this study. It is seen that natural lifetimes are also a very small contribution to the broadening of the Auger peaks. The main parameter for the broadening of the Auger peaks is the response function of the spectrometer.



**Table 1**

Natural widths and lifetimes for the  $1s2s2p^24P$  states for  $O^{5+}$ . Lifetimes for  $2P_{\pm}$  states were taken from Ref. [26] and for  $4P_j$  states from Ref. [24]. Numbers in square brackets stand for powers of 10.

State	Lifetime (ns)	Natural width (eV)
$4P_{1/2}$	0.900	7.31[−7]
$4P_{3/2}$	2.500	2.63[−7]
$2P_{3/2}$	29.57	2.23[−8]
$2P_{-}$	9.44[−5]	6.97[−3]
$2P_{+}$	1.36[−5]	4.84[−2]

Therefore, in the high resolution ZAPS technique the effects of solid angle line broadening and natural width are very small, thus allowing for broadening effects originating from the beam energy width to become measurable. In our SIMION Monte Carlo approach, all the types of broadening are inherently included in the simulation. Thus, by appropriately tuning the beam energy width and comparing the simulations to the corresponding measurements we were able to accurately obtain its value.

## 6. Conclusions

A new technique for accurately determining the energy width,  $\Delta E_p/E_p$ , of the ion beams delivered by tandem Van de Graaff accelerators is presented. The technique is based on the comparison between measurements of high resolution projectile KLL Auger spectra and corresponding Monte Carlo-type simulations obtained within the SIMION simulations ion-optics package. The results of our technique are in good overall agreement with results from nuclear resonance techniques, widely used in nuclear physics experiments. The main advantage of our technique is that it is an in situ approach, since the energy ripple is convoluted within the Auger electron spectra, and thus does not necessitate additional measurements for its determination. We believe that the proposed technique is accurate enough and realistically applicable to be considered as an additional method for ion beam diagnostics.

## CRediT authorship contribution statement

**S. Nanos:** Conceptualization, Methodology, Software, Investigation, Validation, Writing – review & editing. **A. Biniskos:** Methodology, Investigation, Software, Validation. **A. Laoutaris:** Methodology, Software, Investigation, Validation, Writing – review & editing. **M. Andrianis:** Investigation. **T.J.M. Zouros:** Methodology, Validation, Resources, Writing – review & editing. **A. Lagoyannis:** Validation, Resources, Writing – review & editing. **E.P. Benis:** Conceptualization, Methodology, Validation, Resources, Data curation, Writing – original draft, Writing – review & editing, Visualization, Supervision, Project administration.

## Declaration of competing interest

The authors declare that they have no known competing financial interests or personal relationships that could have appeared to influence the work reported in this paper.

## Data availability

Data will be made available on request.

## Acknowledgments

We acknowledge support by the project “Cluster of Accelerator Laboratories for Ion-Beam Research and Applications - CALIBRA” (MIS 5002799), which is implemented under the Action “Reinforcement of the Research and Innovation Infrastructure”, funded by the Operational Programme “Competitiveness, Entrepreneurship and Innovation” (NSRF 2014–2020) and co-financed by Greece and the European Union (European Regional Development Fund).

## References

- [1] H. Betz, Charge states and charge-changing cross sections of fast heavy ions penetrating through gaseous and solid media, *Rev. Modern Phys.* 44 (1972) 465–539, <http://dx.doi.org/10.1103/RevModPhys.44.465>.
- [2] I. Dmitriev, V. Nikolaev, Semi-empirical method for the calculation of the equilibrium distribution of charges in a fast-ion beam, *Sov. Phys. J.* 20 (1964) 409–415.
- [3] R. Sayer, Semi-empirical formulas for heavy-ion stripping data, *Rev. Phys. Appl.* 12 (1977) 1543–1546, <http://dx.doi.org/10.1051/rphysap:0197700120100154300>.
- [4] G. Schiwietz, P. Grande, Improved charge-state formulas, *Nucl. Instrum. Methods Phys. Res. B* 175 (2001) 125–131, [http://dx.doi.org/10.1016/S0168-583X\(00\)00583-8](http://dx.doi.org/10.1016/S0168-583X(00)00583-8).
- [5] K.P. Nesteruk, L. Ramseyer, T. Carzaniga, S. Braccini, Measurement of the beam energy distribution of a medical cyclotron with a multi-leaf faraday cup, *Atoms* 3 (4) <http://dx.doi.org/10.3390/instruments3010004>.
- [6] R. Nazhmudinov, A. Kubankin, P. Karataev, I. Kishin, A. Vukolov, A. Potylitsyn, P. Zhukovaa, V. Nasonova, A multi-wirescanner test setup utilizing characteristic X-rays for charged particle and photon beam diagnostics, *J. Instr.* 13 (12) (2018) P12012, <http://dx.doi.org/10.1088/1748-0221/13/12/P12012>.
- [7] S. Harissopulos, C. Chronidou, K. Spyrou, T. Paradellis, C. Rolfs, W.H. Schulte, H.W. Becker, The  $^{27}\text{Al}(p,\gamma)^{28}\text{Si}$  reaction: direct capture cross-section and resonance strengths at  $E_p = 0.2\text{--}1.12$  MeV, *Eur. Phys. J. A* 9 (2020) 479, <http://dx.doi.org/10.1007/s100500070006>.
- [8] V. Paneta, M. Kokkoris, A. Lagoyannis, K. Preketes-Sigalas, Preketes-sigalas, accurate accelerator energy calibration using selected resonances in proton elastic scattering and in (p,  $\gamma$ ) and (p,  $p'\gamma$ ) reactions, *Nucl. Instrum. Methods Phys. Res. B* 406 (2017) 108–111, <http://dx.doi.org/10.1016/j.nimb.2017.03.040>.
- [9] SIMION, <http://www.simion.com>.
- [10] APAPES, <https://apapes.physics.uoc.gr/>.
- [11] S. Harissopulos, M. Andrianis, M. Axiotis, A. Lagoyannis, A.G. Karydas, Z. Kotsina, A. Laoutaris, G. Apostolopoulos, A. Theodorou, T.J.M. Zouros, I. Madesis, E.P. Benis, The tandem accelerator laboratory of NCSR “Demokritos”: Current status and perspectives, *Eur. Phys. J. Plus* 136 (2021) 617, <http://dx.doi.org/10.1140/epjp/s13360-021-01596-5>.
- [12] A. Laoutaris, Study and Implementation of a System of Ion Post-Strippers for Use at the 5.5 MV Tandem Van de Graaff Accelerator of the National Center for Science and Research “Demokritos” (Master’s thesis), Technical University of Athens and NCSR Demokritos, 2016, unpublished.
- [13] E. Asimakopoulou, I. Madesis, A. Dimitriou, T.J.M. Zouros, T. Mertzimekis, A. Lagoyannis, M. Axiotis, Incorporation of an ion post stripper for the APAPES experimental setup, *HNPS* 22 (2014) 122–125, <http://dx.doi.org/10.12681/hnps.1918>.
- [14] N. Stolterfoht, High resolution Auger spectroscopy in energetic ion atom collisions, *Phys. Rep.* 164 (1987) 315–424, [http://dx.doi.org/10.1016/0370-1573\(87\)90036-6](http://dx.doi.org/10.1016/0370-1573(87)90036-6).
- [15] A. Itoh, N. Stolterfoht, Zero-degree projectile Auger electron spectroscopy in energetic ion-atom collisions, *Nuc. Instr. Meth. Phys. Res. B* 10–11 (1985) 97–103, [http://dx.doi.org/10.1016/0168-583X\(85\)90211-3](http://dx.doi.org/10.1016/0168-583X(85)90211-3).
- [16] I. Madesis, A. Dimitriou, A. Laoutaris, A. Lagoyannis, M. Axiotis, T. Mertzimekis, M. Andrianis, S. Harissopulos, E.P. Benis, B. Sulik, I. Valastyán, T.J.M. Zouros, Atomic physics with accelerators: Projectile electron spectroscopy (APAPES), *J. Phys. Conf. Ser.* 583 (2015) 012014, <http://dx.doi.org/10.1088/1742-6596/583/1/012014>.
- [17] I. Madesis, A. Laoutaris, T.J.M. Zouros, S. Nanos, E.P. Benis, Projectile electron spectroscopy and new answers to old questions: latest results at the new atomic physics beamline in Demokritos, Athens, in: D. Belkić, I. Bray, A. Kadyrov (Eds.), *State-of-the-Art Reviews on Energetic Ion-Atom and Ion-Molecule Collisions*, in: *Interdisciplinary Research on Particle Collisions and Quantitative Spectroscopy*, vol. 2, World Scientific, Singapore, 2019, pp. 1–31 (Chapter 1).
- [18] T.J.M. Zouros, D.H. Lee, Zero degree Auger electron spectroscopy of projectile ions, in: S.M. Shafroth, J.C. Austin (Eds.), *Accelerator-Based Atomic Physics: Techniques and Applications*, AIP, Woodbury, NY, 1997, pp. 426–479 (Chapter 13).
- [19] S. Nanos, M. Quinto, I. Madesis, A. Laoutaris, T.J.M. Zouros, R. Rivarola, J. Monti, E.P. Benis, Subshell contributions to electron capture into the continuum in MeV/u collisions of deuterons with multielectron targets, *Phys. Rev. A* 105 (2022) 022806, <http://dx.doi.org/10.1103/PhysRevA.105.022806>.

- [20] I. Madesis, A. Laoutaris, T.J.M. Zouros, E.P. Benis, J.W. Gao, A. Dubois, Pauli shielding and breakdown of spin statistics in multielectron multi-open-shell dynamical atomic systems, *Phys. Rev. Lett.* 124 (2020) 113401, <http://dx.doi.org/10.1103/PhysRevLett.124.113401>.
- [21] A. Laoutaris, S. Nanos, I. Madesis, S. Passalidis, E.P. Benis, A. Dubois, T.J.M. Zouros, Coherent treatment of transfer-excitation processes in swift ion-atom collisions, *Phys. Rev. A* 106 (2022) 022810, <http://dx.doi.org/10.1103/PhysRevA.106.022810>.
- [22] E.P. Benis, M. Zamkov, P. Richard, T.J.M. Zouros, Technique for the determination of the  $1s2s\ ^3S$  metastable fraction in two-electron ion beams, *Phys. Rev. A* 65 (2002) 064701, <http://dx.doi.org/10.1103/PhysRevA.65.064701>.
- [23] S. Doukas, I. Madesis, A. Dimitriou, A. Laoutaris, T.J.M. Zouros, E.P. Benis, Determination of the solid angle and response function of a hemispherical spectrograph with injection lens for Auger electrons emitted from long lived projectile states, *Rev. Sci. Instrum.* 86 (2015) 043111, <http://dx.doi.org/10.1063/1.4917274>.
- [24] E.P. Benis, S. Doukas, T.J.M. Zouros, F. Parente, C. Martins, J.P. Marques, J.P. Santos, Evaluation of the effective solid angle of a hemispherical deflector analyser with injection lens for metastable Auger projectile states, *Nuc. Instr. Meth. Phys. Res. B* 365 (2015) 457–561, <http://dx.doi.org/10.1016/j.nimb.2015.07.006>.
- [25] S. Nanos, E.P. Benis, Method for determining the lifetimes of the long-lived  $1s2s2p\ ^4P_J$  state J-levels, *AIP Conf. Proc.* 2075 (2019) 200001, <http://dx.doi.org/10.1063/1.5091426>.
- [26] M.H. Chen, B. Crasemann, H. Mark, Deexcitation of light Li-like ions in the  $1s2s2p$  state, *Phys. Rev. A* 27 (1983) 544–547, <http://dx.doi.org/10.1103/PhysRevA.27.544>.